PHYSICAL REVIEW D **96,** 054516 (2017)

# Isospin-0 $\pi\pi$ s-wave scattering length from twisted mass lattice QCD

L. Liu,[1,*] S. Bacchio,[2,3] P. Dimopoulos,[4,5] J. Finkenrath,[6] R. Frezzotti,[7] C. Helmes,[1] C. Jost,[1] B. Knippschild,[1] B. Kostrzewa,[1] H. Liu,[8] K. Ottnad,[1] M. Petschlies,[1] C. Urbach,[1,†] and M. Werner[1]

(ETM Collaboration)

[1]*Helmholz-Institut für Strahlen- und Kernphysik and Bethe Center for Theoretical Physics, Universität Bonn, D-53115 Bonn, Germany*
[2]*Department of Physics, University of Cyprus, PO Box 20537, 1678 Nicosia, Cyprus*
[3]*Fakultät für Mathematik und Naturwissenschaften, Bergische Universität Wuppertal, 42119 Wuppertal, Germany*
[4]*Centro Fermi—Museo Storico della Fisica e Centro Studi e Ricerche Enrico Fermi, Compendio del Viminale, Piazza del Viminiale 1, I-00184 Rome, Italy*
[5]*Dipartimento di Fisica, Università di Roma "Tor Vergata", Via della Ricerca Scientifica 1, I-00133 Rome, Italy*
[6]*Computation-based Science and Technology Research Center, The Cyprus Institute, PO Box 27456, 1645 Nicosia, Cyprus*
[7]*Dipartimento di Fisica, Università and INFN di Roma Tor Vergata, 00133 Roma, Italy*
[8]*Albert Einstein Center for Fundamental Physics, University of Bern, 3012 Bern, Switzerland*
(Received 13 December 2016; published 28 September 2017)

We present results for the isospin-0 $\pi\pi$ s-wave scattering length calculated with Osterwalder-Seiler valence quarks on Wilson twisted mass gauge configurations. We use three $N_f = 2$ ensembles with unitary (valence) pion mass at its physical value (250 MeV), at 240 MeV (320 MeV) and at 330 MeV (400 MeV), respectively. By using the stochastic Laplacian Heaviside quark smearing method, all quark propagation diagrams contributing to the isospin-0 $\pi\pi$ correlation function are computed with sufficient precision. The chiral extrapolation is performed to obtain the scattering length at the physical pion mass. Our result $M_\pi a_0^{I=0} = 0.198(9)(6)$ agrees reasonably well with various experimental measurements and theoretical predictions. Since we only use one lattice spacing, certain systematics uncertainties, especially those arising from unitary breaking, are not controlled in our result.

DOI: 10.1103/PhysRevD.96.054516

## I. INTRODUCTION

Quantum chromodynamics (QCD) is established as the fundamental theory of the strong interactions. QCD at low energies is largely determined by chiral symmetry, which is spontaneously broken. The effective theory of QCD at low energies is chiral perturbation theory ($\chi$PT) [1–3], representing a systematic expansion in the quark masses and momenta. Elastic $\pi\pi$ scattering provides an ideal testing ground for the mechanism of chiral symmetry breaking. Since only the pions—the pseudo-Goldstone bosons of SU(2) chiral symmetry—are involved, the expansion is expected to converge rapidly. In fact, the s-wave scattering length in the weakly repulsive isospin-2 channel can be reproduced by leading order (LO) $\chi$PT [4] with a deviation of only 0.5% when compared to the results obtained from experiments combined with Roy equations [5].

However, in the isospin-0 channel the situation is different: the interaction is attractive and much stronger than in the isospin-2 channel. The agreement between LO $\chi$PT and experiments for the s-wave scattering length in the isospin-0 channel is much less impressive: they deviate by around 30% [4–6]. Moreover, this channel accommodates the lowest QCD resonance—the mysterious $\sigma$ or $f_0(500)$ scalar meson. Although it plays a crucial role in some fundamental features of QCD, its existence was disputed for a long time. Only recently it was established unambiguously with dispersive analyses and new experimental data, see Ref. [7] for a review.

This makes a nonperturbative, *ab initio* computation of $\pi\pi$ interaction properties in the isospin-0 channel directly from QCD highly desirable. Lattice QCD is the only available method to perform such a computation with controlled systematic uncertainties. Lüscher showed that the infinite volume scattering parameters can be related to the discrete spectrum of the eigenstates in a finite-volume box [8,9]. This allows one to compute scattering properties in lattice QCD, which is necessarily implemented in a finite volume and Euclidean space-time.

For the isospin-2 channel, many lattice results have become available. See Refs. [10–13] for the most recent

*liuming@hiskp.uni-bonn.de
†urbach@hiskp.uni-bonn.de

 

ones. For the isospin-0 channel the situation is more complicated mainly due to the fermionic disconnected diagrams contributing here, which are challenging to compute in lattice QCD. To date there are only two full lattice QCD computations dedicated to this channel [11,14]. In Ref. [11], the s-wave scattering length was computed for three unphysically large pion masses. An extrapolation to the physical point was performed to obtain the scattering length at physical pion mass. The authors of Ref. [14] on the other hand extracted many energy eigenstates in the corresponding channel and obtained the scattering amplitudes for two values of pion mass—236 MeV and 391 MeV. The information about the $\sigma$ meson is deduced from the pole structure in the scattering amplitudes at the two unphysical pion masses, respectively.

In this work we compute the scattering length of the isospin-0 $\pi\pi$ channel in twisted mass lattice QCD [15] and Lüscher's finite volume method [8,9]. As discussed in Ref. [16], the explicit isospin breaking of the twisted mass quark action makes it prohibitively complicated to study this channel with this action. To circumvent this complication we use a mixed action approach with Osterwalder-Seiler quarks [17] in the valence sector, which preserves isospin symmetry. This approach introduces additional lattice artefacts due to unitarity breaking. These lattice artefacts are of $\mathcal{O}(a^2)$ and will vanish only in the continuum limit. In particular, due to isospin breaking in the sea there is possibly residual mixing with $I = 2$, $I_z = 0$. Since we use only one value of lattice spacing, systematic uncertainties in our results are not fully controlled. Further calculations are needed to explicitly address these uncertainties. However, they are beyond the scope of this work.

This paper is organized as follows. The lattice setup is discussed in Sec. II. Lüscher's finite volume method is introduced in Sec. III. In Sec. IV we present the computation of the finite volume spectrum of the isospin-0 $\pi\pi$ system. The result for the scattering length is given in Sec. V. The last section is devoted to a brief summary and discussions.

## II. LATTICE ACTION

The results presented in this paper are based on the gauge configurations generated by the European Twisted Mass Collaboration (ETMC) with Wilson clover twisted mass quark action at maximal twist [15]. The gauge action is the Iwasaki gauge action [18]. We use three $N_f = 2$ ensembles with pion mass at the physical value, at 240 MeV and at 330 MeV, respectively. The lattice spacing is $a = 0.0931(2)$ fm for all three ensembles, as found in Ref. [19] up to $\mathcal{O}(a^2)$ lattice artefacts. In Table I we list the three ensembles with the relevant input parameters, the lattice volume and the number of configurations. More details about the ensembles are presented in Ref. [19].

The sea quarks are described by the Wilson clover twisted mass action. The Dirac operator for the light quark doublet consists of the Wilson twisted mass Dirac operator [15] combined with the clover term (in the so-called physical basis)

TABLE I. The gauge ensembles used in this study. The labeling of the ensembles follows the notations in Ref. [19,20]. In addition to the relevant input parameters we give the lattice volume $(L/a)^3 \times T/a$ and the number of evaluated configurations $N_{\mathrm{conf}}$.

| ensemble | $\beta$ | $c_{\mathrm{sw}}$ | $a\mu_\ell$ | $(L/a)^3 \times T/a$ | $N_{\mathrm{conf}}$ |
|---|---|---|---|---|---|
| *cA*2.09.48 | 2.10 | 1.57551 | 0.009 | $48^3 \times 96$ | 615 |
| *cA*2.30.48 | 2.10 | 1.57551 | 0.030 | $48^3 \times 96$ | 352 |
| *cA*2.60.32 | 2.10 | 1.57551 | 0.060 | $32^3 \times 64$ | 337 |

$$D_\ell = \tilde{\nabla} - i\gamma_5\tau_3\left[W_{\mathrm{cr}} + \frac{i}{4}c_{\mathrm{sw}}\sigma^{\mu\nu}\mathcal{F}^{\mu\nu}\right] + \mu_\ell, \qquad (1)$$

with $\tilde{\nabla} = \gamma_\mu(\nabla^*_\mu + \nabla_\mu)/2$, $\nabla_\mu$ and $\nabla^*_\mu$ the forward and backward lattice covariant derivatives. Here $c_{sw}$ is the so-called Sheikoleslami-Wohlert improvement coefficient [21] multiplying the clover term and $W_{\mathrm{cr}} = -ra\nabla^*_\mu\nabla_\mu + m_{\mathrm{cr}}$, with $m_{\mathrm{cr}}$ the critical mass. $\mu_\ell$ is the average up/down (twisted) quark mass. $a$ is the lattice spacing and $r = 1$ the Wilson parameter. $D_\ell$ acts on a flavor doublet spinor $\psi_\ell = (u, d)^T$. In our case the clover term is not used for $\mathcal{O}(a)$ improvement but serves to significantly reduce the effects of isospin breaking [19].

The critical mass has been determined as described in Refs. [20,22]. This guarantees automatic $\mathcal{O}(a)$ improvement [23], which is one of the main advantages of the Wilson twisted mass formulation of lattice QCD.

In the valence sector we introduce quarks in the so-called Osterwalder-Seiler (OS) discretization [17]. The corresponding *up* and *down* single flavor lattice Dirac operators read

$$D^\pm_\ell = \tilde{\nabla} \pm i\gamma_5\left[W_{\mathrm{cr}} + \frac{i}{4}c_{\mathrm{sw}}\sigma^{\mu\nu}\mathcal{F}^{\mu\nu}\right] + \mu^{\mathrm{OS}}_\ell. \qquad (2)$$

From this definition it is apparent that OS *up* and *down* quarks have explicit SU(2) isospin symmetry if for both e.g. $D^+_\ell$ was used. The matching of OS to unitary actions is performed by matching the quark mass values, i.e. $\mu^{\mathrm{OS}}_\ell = \mu_\ell$. The value of $m_{\mathrm{cr}}$ in the OS action can be shown to be identical to the unitary one and $\mathcal{O}(a)$ improvement stays valid [17]. Moreover, we have shown in Ref. [24] that in such a mixed action approach disconnected contributions to $\eta$ and $\eta'$ mesons can be computed and the results agree with the unitary ones [25] in the continuum limit. Therefore, this mixed action approach should works also in the case of $\pi\pi$ scattering, where disconnected contributions can be expected to be less important, since OZI suppression is in place. However, there is a potential complication arising from the double poles in flavor-neutral

meson propagators present in a quenched or partially quenched theory [26]. The scalar correlators with disconnected diagrams suffer from unphysical contributions due to the double poles. The unphysical contributions to the $a_0$ and $\pi\pi$ correlators have been studied in Refs. [27–30]. In this work, we are not going to consider this problem since the formula of these unphysical contributions for our partially quenched approach is not available. Also, as will be presented in Sec. IV, our numerical results do not indicate large unphysical contributions. All the correlators we computed numerically are positive within the obtained statistics and are well described by a single exponential function of $t/a$ in a reasonably large time range. This would not be the case if there were large unphysical contributions as shown in Refs. [27–30]. Nevertheless, one should keep in mind that the effects of the double poles may cause uncertainties that are not considered in our results.

Masses computed with OS valence quarks differ from those computed with twisted mass valence quarks by lattice artefact of $\mathcal{O}(a^2)$, in particular

$$(M_\pi^{\mathrm{OS}})^2 - (M_\pi)^2 = \mathcal{O}(a^2).$$

For twisted clover fermions this difference is much reduced as compared to twisted mass fermions [19], however, the effect is still sizable. We use the OS pion mass in this paper, with the consequence that the pion mass value of the cA2.09.48 ensemble takes a value larger (around 250 MeV) than the physical one.

As a smearing scheme we use the stochastic Laplacian Heavyside (sLapH) method [31,32] for our computation. The details of the sLapH parameter choices for a set of $N_f = 2 + 1 + 1$ Wilson twisted mass ensembles are given in Ref. [13]. The parameters for the ensembles used in this work are the same as those for $N_f = 2 + 1 + 1$ ensembles with the corresponding lattice volume.

## III. LÜSCHER'S FINITE VOLUME METHOD

Lüscher's finite volume method provides a direct relation between the energy eigenvalues of a two-particle system in a finite box and the scattering phase shift of the two particles in the infinite volume. Considering two particles with mass $m_1$ and $m_2$ in a cubic box of size $L$, the energy of this system in the center-of-mass frame reads

$$E = \sqrt{m_1^2 + \vec{k}^2} + \sqrt{m_2^2 + \vec{k}^2}, \tag{3}$$

where $\vec{k}$ is the scattering momentum. For the following discussion, it is convenient to define a dimensionless variable $q$ via

$$q^2 = \frac{\vec{k}^2 L^2}{(2\pi)^2}, \tag{4}$$

which differs from an integer due to the interaction of the two particles.

The general form of Lüscher's formula reads [9]:

$$\det\left[e^{2i\delta_l}\delta_{ll'}\delta_{nn'} - \frac{\mathcal{M}^{\Gamma}_{ln,l'n'} + i}{\mathcal{M}^{\Gamma}_{ln,l'n'} - i}\right] = 0, \tag{5}$$

where $\delta_l$ is the phase shift of the partial wave with angular momentum $\{l\}$, $\Gamma$ denotes an irreducible representation (irrep) of the cubic group. The matrix in the determinant is labeled by the pair $(l, n)$, in which $\{l\}$ are the angular momenta subduced into the irrep $\Gamma$ and $n$ is an index indicating the $n^{th}$ occurrence of that $l$ in the irrep. The matrix element $\mathcal{M}^{\Gamma}_{ln,l'n'}$ is a complicated function of $q$ but can be computed numerically.

In this work we are interested in the s-wave low energy scattering in the isospin-0 $\pi\pi$ channel. Therefore, we will compute only the lowest energy level in the center-of-mass frame. In this case one should consider the irrep $A_1^+$. Assuming that the effects of the partial waves with $l \geq 4$ are negligible, the matrix in the determinant of Eq. (5) becomes one-dimensional and the equation reduces to

$$q \cot \delta_0(k) = \frac{\mathcal{Z}_{00}(1; q^2)}{\pi^{3/2}}, \tag{6}$$

where $\mathcal{Z}_{00}(1; q^2)$ is the Lüscher zeta-function which can be evaluated numerically for given value of $q^2$. Using the effective range expansion of s-wave elastic scattering near threshold, we have

$$k \cot \delta_0(k) = \frac{1}{a_0} + \frac{1}{2} r_0 k^2 + \mathcal{O}(k^4), \tag{7}$$

where $a_0$ is the scattering length and $r_0$ is the effective range parameter. Once the finite volume energy $E$ is determined from lattice QCD simulations, the scattering length $a_0$ can be calculated from the following relation

$$\frac{2\pi}{L}\frac{\mathcal{Z}_{00}(1; q^2)}{\pi^{3/2}} = \frac{1}{a_0} + \frac{1}{2} r_0 k^2 + \mathcal{O}(k^4). \tag{8}$$

It should be pointed out that Lüscher's formulas presented here, i.e. Eqs. (5) and (6), are for the scattering processes with $k^2 > 0$. The phase shift $\delta_0(k)$ in the continuum is only defined for positive $k^2$. In the case of negative $k^2$, one can introduce a phase $\sigma_0(k)$ which is related to $\delta_0(k)$ by analytic continuation of $\tan \sigma_0(k) = -i \tan \delta_0(k)$ [9]. Only when there is a bound state at the corresponding energy, the phase $\sigma_0(k)$ has physical interpretation and its value equals to $-\pi/4$ (modulo $\pi$) in the continuum and infinite volume limit. For the purpose of this paper—calculating the scattering length, we will only consider the lowest energy level in the center-of-mass frame. Since the interaction in the isospin-0

$\pi\pi$ channel is attractive, this energy level is below the threshold, i.e. $k^2 < 0$. For convenience, in the following we will always use the notation $k \cot \delta_0(k)$, which is understood as the analytically continued form for $k^2 < 0$. Please note that Eq. (8) holds for both positive and negative $k^2$ as long as the modulus of $k^2$ is close to zero.

## IV. FINITE VOLUME SPECTRUM

In lattice QCD, the discrete spectra of hadronic states are extracted from the correlation functions of the interpolating operators that resemble the states. Due to the isospin symmetry breaking of the twisted mass quark action, it is difficult to investigate the isospin-0 $\pi\pi$ channel directly in unitary twisted mass lattice QCD [16]. For this reason we use a mixed action approach with the OS action [17] in the valence sector and choose $D_\ell^+$ in Eq. (2) for both *up* and *down* quarks, so that the isospin symmetry is guaranteed in the valence sector. In this section we describe our methodology to calculate the energies of the isospin-0 $\pi\pi$ system.

### A. Computation of the correlation functions

We define the interpolating operator that represents the isospin-0 $\pi\pi$ state in terms of OS valence quarks

$$\mathcal{O}_{\pi\pi}^{\mathrm{I}=0}(t) = \frac{1}{\sqrt{3}}(\pi^+\pi^-(t) + \pi^-\pi^+(t) + \pi^0\pi^0(t)), \quad (9)$$

with single pion operators summed over spatial coordinates $\mathbf{x}$ to project to zero momentum

$$\begin{aligned}\pi^+(t) &= \sum_{\mathbf{x}} \bar{d}\,\gamma_5 u(\mathbf{x}, t),\\ \pi^-(t) &= \sum_{\mathbf{x}} \bar{u}\,\gamma_5 d(\mathbf{x}, t),\\ \pi^0(t) &= \sum_{\mathbf{x}} \frac{1}{\sqrt{2}}(\bar{u}\gamma_5 u - \bar{d}\gamma_5 d)(\mathbf{x}, t).\end{aligned} \quad (10)$$

Here $u$ and $d$ represent the OS *up* and *down* quarks, respectively. With OS valence quarks all three pions are mass degenerate and will be denoted as $M_\pi^{\mathrm{OS}}$.

The energy of the isospin-0 $\pi\pi$ state can be computed from the exponential decay in time of the correlation function

$$C_{\pi\pi}(t) = \frac{1}{T}\sum_{t_{src}=0}^{T-1} \langle \mathcal{O}_{\pi\pi}^{\mathrm{I}=0}(t + t_{src})(\mathcal{O}_{\pi\pi}^{\mathrm{I}=0})^\dagger(t_{src})\rangle, \quad (11)$$

where $T$ is the temporal lattice extend. The four diagrams contributing to this correlation function, namely the direct connected diagram $D(t)$, the cross diagram $X(t)$, the box diagram $B(t)$ and the vacuum diagram $V(t)$, are depicted in Fig. 1(a)–(d). The correlation function can be expressed in terms of all relevant diagrams as

$$C_{\pi\pi}(t) = 2D(t) + X(t) - 6B(t) + 3V(t). \quad (12)$$

$C_{\pi\pi}$ and the contributions from individual diagrams $D$, $X$, $B$ and $V$ are plotted in Fig. 2 for the three ensembles.

Even though we have full SU(2) isospin symmetry in the valence sector when using OS valence quarks as described above, we have to consider effects of unitarity breaking. This may in particular happen due to the vacuum diagram $V(t)$. There is no symmetry available to prevent this diagram to couple for instance to intermediate states of $n \geq 1$ unitary neutral pions (the neutral pion has vacuum quantum numbers in maximally twisted mass lattice QCD), since parity is not a good quantum number for our action. Since the neutral pion is the lightest meson in the spectrum with Wilson twisted mass fermions at finite value of the lattice spacing, the appearance of such states with $n = 1$ (and maybe $n = 2$) will dominate the large Euclidean time behavior of the correlation function $C_{\pi\pi}$, if the overlap of the used interpolating operators with these states is non-zero. In order to resolve this mixing, we build a $2 \times 2$ matrix of correlation functions

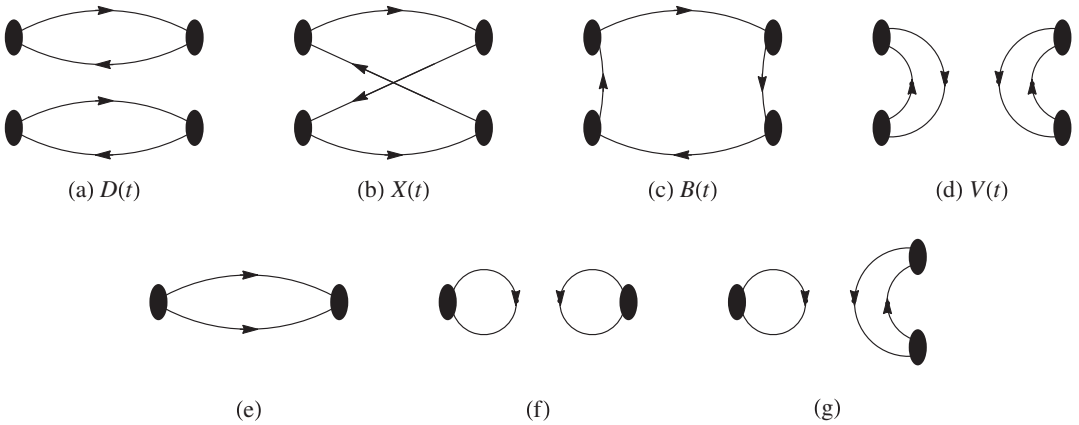


FIG. 1. Diagrams contributing to the correlation functions. (a)–(d) represent the usual contributions to $C_{\pi\pi}$, while (e)–(f) need to be taken into account due to unitarity breaking effects.

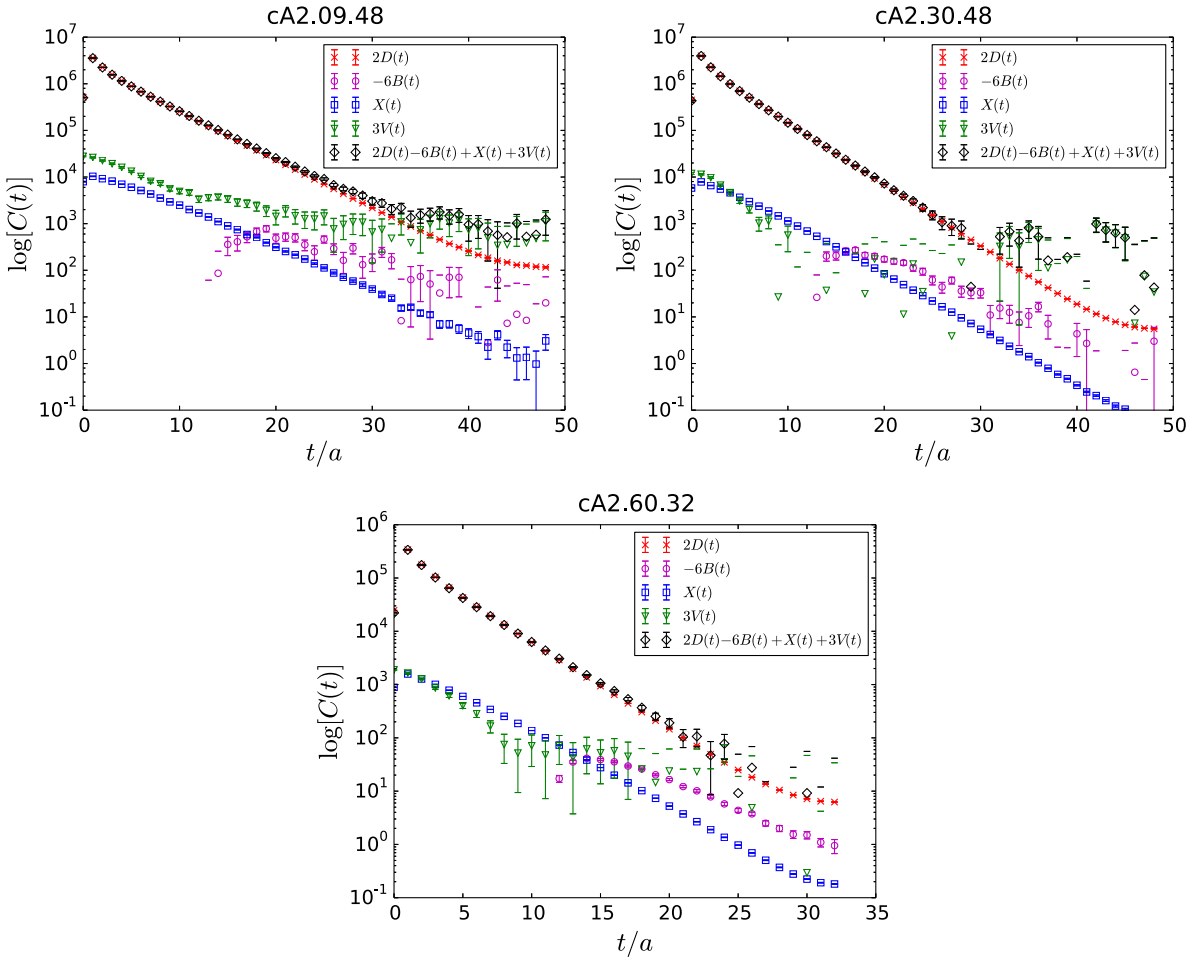


FIG. 2. Correlation functions of the operator $\mathcal{O}^{\mathrm{I}=0}_{\pi\pi}$ and the single diagrams $D$, $X$, $B$, $V$ for the three ensembles listed in Table I.

$$C_{ij}(t) = \frac{1}{T}\sum_{t_{src}=0}^{T-1} \langle \mathcal{O}_i(t+t_{src})\mathcal{O}_j^{\dagger}(t_{src})\rangle \tag{13}$$

with $i$, $j$ labeling the operator $\mathcal{O}^{\mathrm{I}=0}_{\pi\pi}$ and the unitary neutral pion operator

$$\pi^{0,uni}(t) = \sum_{\mathbf{x}} \frac{1}{\sqrt{2}}(\bar{u}\gamma_5 u - \bar{d}'\gamma_5 d')(\mathbf{x},t), \tag{14}$$

where $u$ and $d'$ are the (unitary) Wilson clover twisted mass *up* and *down* quarks. We use $d'$ to distinguish it from OS *down* quark in Eq. (10). The twisted mass *up* quark coincides with the OS *up* quark with our matching scheme of the OS to the unitary action.

The diagrams contributing to the correlation function of the unitary neutral pion operator are depicted in Fig. 1(e)–(f). The two operators couple solely via the vacuum diagram, see Fig. 1(g).

The computation of the disconnected diagrams, e.g. Fig. 1(c), (d), (f), and (g), requires the quark propagator from a time slice $t$ to the same time for every $t$. This has been a challenge in lattice QCD for decades. By using the stochastic LapH quark smearing method [31,32], we have all-to-all propagators available. The disconnected diagrams can be computed directly from those propagators.

We can reduce lattice artefacts in the vacuum diagrams following the ideas worked out in Ref. [24]. In the continuum limit the difference between $u_+$ ($d_+$) quarks corresponding to $D^+_\ell$ and $u_-$ ($d_-$) quarks corresponding to $D^-_\ell$ vanishes [17]. Therefore, we can write

$$\begin{aligned}\mathcal{O}(a) &= \langle \bar{u}_+ d_+(x)\bar{d}_+ u_+(y) - \bar{u}_- d_-(x)\bar{d}_- u_-(y)\rangle \\ &= \mathrm{Tr}\{S^+(x,y)S^+(y,x)\} - \mathrm{Tr}\{S^-(x,y)S^-(y,x)\} \\ &= \mathrm{Tr}\{S^+(x,y)S^+(y,x)\} - \mathrm{Tr}\{(S^+(x,y)S^+(y,x))^{\dagger}\} \\ &= 2i\mathrm{Im}\mathrm{Tr}\{S^+(x,y)S^+(y,x)\},\end{aligned}$$

where $S^{\pm} \equiv (D^{\pm}_\ell)^{-1}$ are the OS quark propagators and we have used $(S^+)^{\dagger} = \gamma_5 S^- \gamma_5$. This shows that the imaginary part of the loop needed in the contraction of the vacuum diagram $V$ is a pure lattice artefact and we will drop it in the

computation. The same argument holds for the vacuum diagrams shown in Fig. 1(f) and (g).

### B. Determination of the energies

Due to the finite temporal extend $T$ of the lattice, the correlation functions of multiparticle operators are polluted by so-called thermal states [33]. In the case of interest here, there is a constant contribution to $C_{\pi\pi}(t)$ of the form

$$\propto |\langle \pi^{\pm,0}|\mathcal{O}^{I=0}_{\pi\pi}|\pi^{\pm,0}\rangle|^2 \cdot e^{-M^{\mathrm{OS}}_{\pi} T},$$

which vanishes in the infinite volume limit $T \to \infty$. However, at finite $T$-values it will dominate the correlation function at large Euclidean time. To remove this artefact we define a shifted correlation matrix

$$\tilde{C}(t) = C(t) - C(t + \delta t). \tag{15}$$

The new matrix $\tilde{C}$ is then free of any constant pollution from the thermal states. The value of $\delta t$ can be adjusted for optimal results. We take $\delta t = 4$ in our analysis. Note that the shifting procedure also subtracts any constants stemming from vacuum expectation values.

The energy levels can then be obtained by solving the generalized eigenvalue problem (GEVP) [34]

$$\tilde{C}(t) v_n(t, t_0) = \lambda_n(t, t_0) \tilde{C}(t_0) v_n(t, t_0). \tag{16}$$

The eigenvalues $\lambda_n(t, t_0)$ are expected to have the following time dependence

$$\lambda_n(t, t_0) = A_n \sinh\left[\left(\frac{T}{2} - t - \frac{\delta t}{2}\right) E_n\right]. \tag{17}$$

The sinh-like behavior comes from the shifting of the correlation functions in Eq. (15). The energies $E_n$ are then obtained by fitting the above functional form to the eigenvalues $\lambda_n(t, t_0)$ in the range where the effective energy shows a plateau. The value of $t_0$ should be chosen such that the correlation function at $t_0$ is dominated by the states we are interested in. We tried various $t_0$ values in the range of 1 to 7 and found negligible differences in the energies. In the following we set $t_0 = 1$. With the two operators used here, we obtain two energy levels, one of which is far below the other one. The lower one agrees with the unitary neutral pion mass, while the higher one is close to $2M^{\mathrm{OS}}_{\pi}$. Hence, we identify the higher one to be the isospin-0 $\pi\pi$ state. In principle, multi neutral and charged unitary pion states could also appear in the spectrum. To resolve these states, more operators need to be included. We have tried so and merely found increased statistical errors of the $I = 0$ $\pi\pi$ state. Therefore, we cannot finally exclude possible contaminations from such states.

As an example, the effective energies of the two eigenvalues for ensemble cA2.09.48 are shown in Fig. 3(a). The fitted energies and fit ranges are indicated by the grey bands in the plot.

To further improve our results we adopt a method to remove the excited state contaminations [35], which we have recently used successfully to study $\eta$ and $\eta'$ mesons [25,36]. It is based on the assumption that vacuum diagrams are only sizeable for low lying states, but negligible for higher excited states. Of course, the validity of this assumption must be checked in the Monte-Carlo data. In our case we know there is a very sizable disconnected contribution to the unitary neutral pion, which represents a pure lattice artefact [37]. A similar contribution has not been found to any other unitary correlation

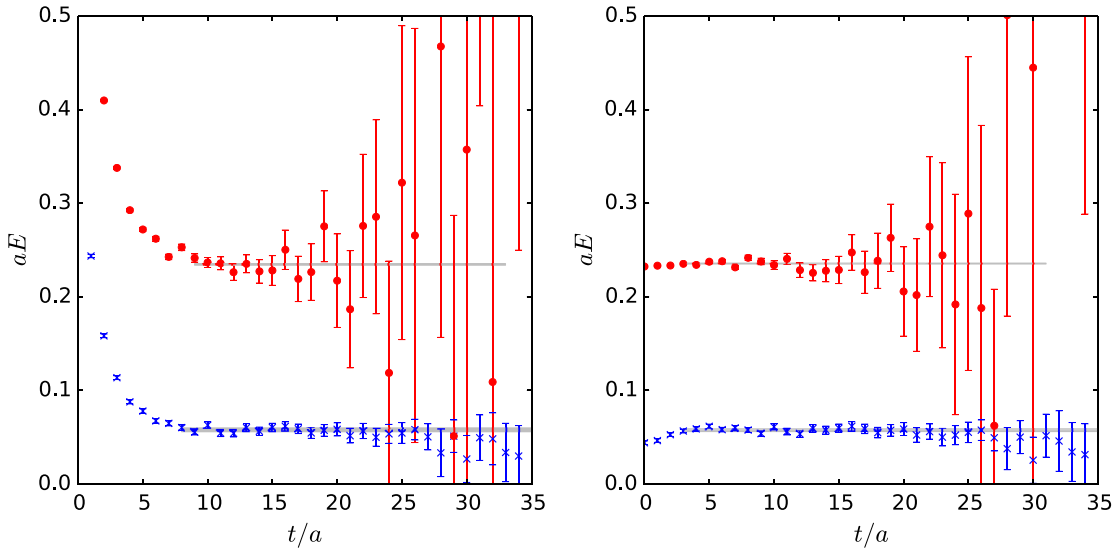


FIG. 3. Effective energies for the ensemble cA2.09.48. The grey bars indicate the fitted values of the energies and the fit ranges. The left and right panels correspond to before and after removing the excited state contaminations, respectively.

function. For the $\pi\pi$ correlation function there are indications that the disconnected contribution is already small by itself [11].

The connected contractions contributing to $\tilde{C}$ are computed with sufficient precision, so we can reliably determine the ground states in the connected correlators and subtract the excited state contributions. We then build a correlation matrix $\tilde{C}^{\mathrm{sub}}$ from the subtracted connected and the original disconnected correlators. If disconnected contributions were relevant only for the ground states, one should find—after diagonalizing $\tilde{C}^{\mathrm{sub}}$—a plateau for both states from small values of $t$ on. Note that with this procedure only the small $t$ behavior of the correlation functions is altered.

To be more specific, the connected contributions to the correlation function $C_{\pi\pi}(t)$ is given by

$$C^{\mathrm{con}}_{\pi\pi}(t) = 2D(t) + X(t) - 6B(t). \tag{18}$$

We fit the functional form Eq. (17) to the shifted correlator $\tilde{C}^{\mathrm{con}}_{\pi\pi}(t) = C^{\mathrm{con}}_{\pi\pi}(t) - C^{\mathrm{con}}_{\pi\pi}(t-\delta t)$. After obtaining the parameters $A$ and $E^{\mathrm{con}}_{\pi\pi}$ from the fit, the connected correlator is reconstructed as

$$\tilde{C}^{\mathrm{con,sub}}_{\pi\pi}(t) = A \sinh\left[\left(\frac{T}{2} - t - \frac{\delta t}{2}\right) E^{\mathrm{con}}_{\pi\pi}\right], \tag{19}$$

in which the excited state contaminations are subtracted. We repeat the fit to the data of $\tilde{C}^{\mathrm{con}}_{\pi\pi}(t)$ for many different fit ranges. The expectation values of the fit parameters are computed as the weighted median over these many fits [13]. By doing this, the systematics arising from different fit ranges is expected to be taken into account. The full correlator is then given by $\tilde{C}^{\mathrm{sub}}_{\pi\pi}(t) = \tilde{C}^{\mathrm{con,sub}}_{\pi\pi}(t) + 3\tilde{V}(t)$, where $\tilde{V}(t)$ is the shifted vacuum correlator $\tilde{V}(t) = V(t) - V(t+\delta t)$. The same procedure is performed for the unitary $\pi^0$ correlation function.

In Fig. 3(b), we present the effective energies of the two eigenvalues of the subtracted correlator matrix $\tilde{C}^{\mathrm{sub}}$ for the same ensemble as in Fig. 3(a). Clearly a plateau appears at much earlier $t$-value compared to Fig. 3(a), while the fitted energies agree very well. Therefore, we use this procedure —which allows us to determine in particular the interacting energy $E_{\pi\pi}$ with much higher accuracy—for the results presented here.

The effective energies after removing the exited states for the ensembles $cA2.30.48$ and $cA2.60.32$ are shown in Fig. 4. In Table II, we collect the values of $E_{\pi\pi}$ and the unitary $\pi^0$ mass $M_{\pi^0}$ obtained from the procedure described above. The unitary charged pion mass $M_{\pi^\pm}$ and the OS pion mass $M_\pi^{\mathrm{OS}}$ are added for convenience.

In order to estimate possible artefacts from the mixing with the unitary $\pi^0$, we also determined the energy $\hat{E}_{\pi\pi}$ by fitting to only the single correlator $\tilde{C}^{\mathrm{sub}}_{\pi\pi}(t)$, without including the operator for the unitary neutral pion. The values are given in the last column of Table II. One can see that the mean value of $\hat{E}_{\pi\pi}$ is slightly lower than $E_{\pi\pi}$ for all three ensembles, but they agree very well with each other considering the statistical error. Keeping in mind that $\pi^0$ mixing is purely a lattice artefact, the agreement between $E_{\pi\pi}$ and $\hat{E}_{\pi\pi}$ indicates that we are not likely to suffer severe lattice artefact here. This can be also seen in the small mass splitting between the unitary charged and neutral pions.

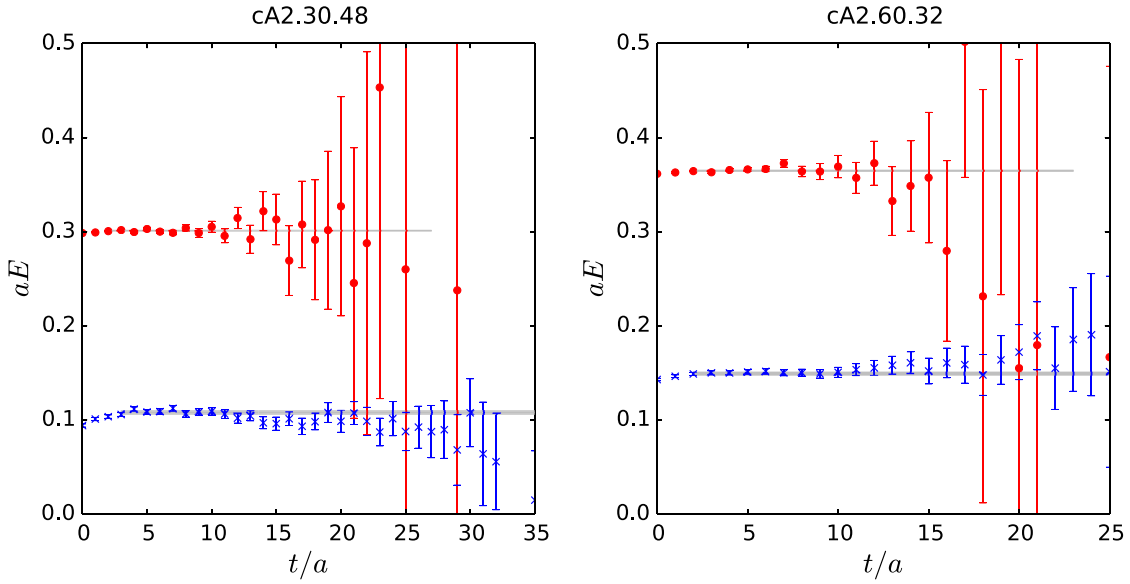


FIG. 4. Effective energies after removing the excited states contaminations for the ensembles $cA2.30.48$ and $cA2.60.32$.

TABLE II. Pion masses and the $\pi\pi$ interacting energies in lattice units for the three ensembles.

| Ensemble | $aM_{\pi^\pm}$ | $aM_{\pi^0}$ | $aM_\pi^{\mathrm{OS}}$ | $aE_{\pi\pi}$ | $a\hat{E}_{\pi\pi}$ |
|---|---|---|---|---|---|
| *cA*2.09.48 | 0.06212(6) | 0.058(2) | 0.11985(15) | 0.2356(4) | 0.2350(4) |
| *cA*2.30.48 | 0.11197(7) | 0.108(2) | 0.15214(11) | 0.3010(3) | 0.3009(3) |
| *cA*2.60.32 | 0.15781(15) | 0.149(2) | 0.18844(24) | 0.3647(5) | 0.3645(5) |

## V. RESULTS

### A. Scattering length

The scattering momentum $k^2$ is calculated from Eq. (3) with the energies $E_{\pi\pi}$ and the OS pion masses listed in Table II. Then the scattering length can be obtained from Eq. (8). Considering the relatively strong interaction in the isospin-0 $\pi\pi$ channel, one has to investigate the contribution of $\mathcal{O}(k^2)$ and higher order terms in the effective range expansion. Since we only have one energy level for each pion mass, we are not able to determine the effective range $r_0$ with our lattice simulations. We rely on the $r_0$ values determined from $\chi$PT [2]. See Appendix A for the details of the $r_0$ values used in our analysis.

The values of $k^2$, $k\cot\delta(k)$ and $\frac{1}{2}r_0k^2$ in lattice units for all three ensembles are given in Table III. For the ensembles *cA*2.09.48 and *cA*2.30.48 the scattering momentum is small due to the large volume. Therefore, the contribution of $\frac{1}{2}r_0k^2$ is expected to be small. As visible from Table III, the value of $\frac{1}{2}r_0k^2$ is indeed less than 3% of $k\cot\delta(k)$ for these two ensembles. We compute the scattering length from Eq. (8) by ignoring the $\mathcal{O}(k^4)$ term, which is well justified for the ensembles *cA*2.09.48 and *cA*2.30.48. The values of $M_\pi^{\mathrm{OS}}a_0^{\mathrm{I}=0}$ for these two ensembles are also given in Table III. The first error is the statistical error and the second error comes from the uncertainty of the effective range $r_0$.

As for the ensemble cA2.60.32, the value of $\frac{1}{2}r_0k^2$ is rather large compared to $k\cot\delta(k)$. This indicates that the effective range expansion up to $\mathcal{O}(k^2)$ might not be a good approximation and the $\mathcal{O}(k^4)$ term might not be negligible. Since the contribution of $\mathcal{O}(k^4)$ is unclear, we refrain from giving the scattering length for this ensemble. There are two possible reasons for the invalidity of the effective range expansion. First, due to the relatively small volume of the ensemble cA2.60.32, the value of $k^2$ is not small enough to make the expansion converge rapidly. Second, at the pion mass around 400 MeV, which is the OS pion mass of the ensemble cA2.60.32, there might be virtual or bound state poles appearing in the isospin-0 $\pi\pi$ scattering amplitude [38–43]. The appearance of such states will give a very large scattering length—positively (negatively) large if it was a virtual (bound) state. Hence, the leading order in the effective range expansion, i.e. $\frac{1}{a_0}$, becomes very small compared to the higher orders. In this case the NLO term $\frac{1}{2}r_0k^2$ can contribute significantly compared to the LO term even when $k^2$ is small. Assuming that the contribution of $\mathcal{O}(k^4)$ term is not bigger than the $\mathcal{O}(k^2)$ term, we can qualitatively estimate the scattering length for this ensemble to be a very large positive number, which features a virtual state. However, we do not exclude the possibility of a bound state because we do not include single meson operators when we compute the matrix of correlation functions. Including these operators might change the resulting spectrum and thus the scattering length.

### B. Chiral extrapolation

In order to obtain the scattering length at the physical pion mass, one needs to perform a chiral extrapolation. $\pi\pi$ scattering has been studied extensively in $\chi$PT in the literature [2,4,44–46]. Since we only have two data points, we fit the NLO $\chi$PT formula, which contains one free parameter, to our data. When expressed in terms of $M_\pi$ and $f_\pi$ computed from lattice simulations, the formula reads [11]

$$M_\pi a_0^{\mathrm{I}=0} = \frac{7M_\pi^2}{16\pi f_\pi^2}\left[1 - \frac{M_\pi^2}{16\pi^2 f_\pi^2}\left(9\ln\frac{M_\pi^2}{f_\pi^2} - 5 - \ell_{\pi\pi}^{\mathrm{I}=0}\right)\right], \tag{20}$$

where $\ell_{\pi\pi}^{\mathrm{I}=0}$ is a combination of the low energy coefficients $\bar{l}_i$'s:

TABLE III. The values of squared scattering momentum $k^2$, $k\cot\delta(k)$, $\frac{1}{2}r_0k^2$ (see appendix), $M_\pi^{\mathrm{OS}}a_0^{\mathrm{I}=0}$ and $M_\pi^{\mathrm{OS}}/f_\pi^{\mathrm{OS}}$ for the three considered ensembles. Values for $k^2$, $k\cot\delta$ and $r_0k^2$ are in lattice units. The first error is the statistical error, the second error comes from the uncertainty of $r_0$, see Appendix A.

| Ensemble | $(ak)^2$ | $ak\cot\delta(k)$ | $\frac{1}{2}ar_0k^2$ | $M_\pi^{\mathrm{OS}}a_0^{\mathrm{I}=0}$ | $M_\pi^{\mathrm{OS}}/f_\pi^{\mathrm{OS}}$ |
|---|---|---|---|---|---|
| *cA*2.09.48 | −0.00049(4) | 0.168(19) | 0.0037(3)(2) | 0.730(83)(1) | 1.86(2) |
| *cA*2.30.48 | −0.00050(4) | 0.167(19) | 0.0042(3)(2) | 0.94(11)(0) | 2.21(1) |
| *cA*2.60.32 | −0.00224(9) | 0.074(7) | 0.0224(9)(22) | – | 2.63(1) |

$$\ell^{\mathrm{I}=0}_{\pi\pi} = \frac{40}{21}\bar{l}_1 + \frac{80}{21}\bar{l}_2 - \frac{5}{7}\bar{l}_3 + 4\bar{l}_4 + 9\ln\frac{M_\pi^2}{f^2_{\pi,phy}}. \quad (21)$$

In this expression, the renormalization scale is set to be the physical pion decay constant $f_{\pi,phy}$. Note that we work in the normalization with $f_{\pi,phy} = 130.4$ MeV. By using the formula in Eq. (20), we have ignored the effects of unitarity breaking. In principle, we should use mixed action $\chi$PT to perform the chiral extrapolation. The $\chi$PT for the mixed action with twisted mass sea quarks and OS valence quarks is presented in Ref. [47]. However, using the two data points at one value of lattice spacing, we are not able to implement the mixed action $\chi$PT formula. With this caveat in mind, we proceed with our analysis.

The OS pion decay constant $f_\pi^{\mathrm{OS}}$ has not been determined by ETMC yet. We compute $f_\pi^{\mathrm{OS}}$ for the three ensembles used in this paper. The values of $M_\pi^{\mathrm{OS}}/f_\pi^{\mathrm{OS}}$ are collected in the last column of Table III. The details of their computation are presented in Appendix B. We recall that the OS pion mass values are larger than their unitary counterpart, see Table II, such that our lowest OS pion mass value is at around 250 MeV.

The method we are applying here is valid only in the elastic region. Therefore, the pion mass values must be small enough to be below threshold where the $\sigma$ meson becomes stable. This threshold is not known exactly, but results obtained with the 1-loop inverse amplitude method [40] (see also Refs. [38,39,48]) suggest that $M_\pi < 400$ MeV should be safe [41]. Our two data points are obtained at pion mass around 250 MeV and 320 MeV respectively, both are below this threshold. Furthermore, the pion mass value should also be small enough to make the chiral expansion valid. To be safe, we perform the chiral extrapolation using only the data point with the lower pion mass (250 MeV). The results of this extrapolation are given in Table IV as fit-1 and illustrated in Fig. 5. The results of the fit with the two data points, which

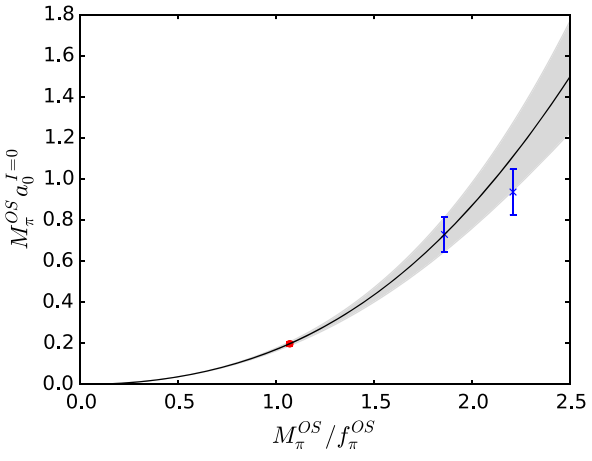


FIG. 5. Chiral extrapolation using only the data point with lower pion mass. The grey band represents the uncertainty. The red point indicates the extrapolated value at physical pion mass.

TABLE IV. Results of the NLO chiral fit. fit-1 includes only one data point, namely cA2.09.48, while fit-2 includes both, cA2.09.48 and cA2.30.48.

| | fit-1 | fit-2 |
|---|---|---|
| $M_\pi a_0^{\mathrm{I}=0}$ (Phy.) | 0.198(9) | 0.192(5) |
| $\ell^{\mathrm{I}=0}_{\pi\pi}$ | 30(8) | 24(4) |
| $\chi^2$/dof | – | 0.75/1 |

TABLE V. Comparison of results available in the literature for $M_\pi a_0^{\mathrm{I}=0}$ and $\ell^{\mathrm{I}=0}_{\pi\pi}$.

| | $M_\pi a_0^{\mathrm{I}=0}$ | $\ell^{\mathrm{I}=0}_{\pi\pi}$ |
|---|---|---|
| This work | 0.198(9)(6) | 30(8)(6) |
| Fu [11] | 0.214(4)(7) | 43.2(3.5)(5.6) |
| Weinberg [4] | 0.1595(5) | – |
| CGL [46] | 0.220(5) | 48.5(4.3) |
| NA48/2 [5] | 0.220(3)(2) | |
| E865 [6] | 0.216(13)(2) | 45.0(11.2)(3.5) |

are given in Table IV as fit-2, agree with fit-1 within errors. We take the difference as an estimate of the systematics arising from chiral extrapolation. This leads to our final result for the scattering length:

$$M_\pi a_0^{\mathrm{I}=0} = 0.198(9)_{\mathrm{stat}}(6)_{\mathrm{sys}}. \quad (22)$$

We remark here that the extrapolation is strongly constrained since $M_\pi^{\mathrm{OS}} a_0^{I=0}$ must vanish in the chiral limit. This explains the small statistical uncertainty on the value extrapolated to the physical point.

We compare our result in Table V to other results available in the literature. Our result for $M_\pi a_0^{I=0}$ is lower, but within errors still compatible with most recent experimental, lattice and Roy equations results. Due to our comparably low value for $M_\pi a_0^{I=0}$, the value for $\ell^{I=0}_{\pi\pi}$ is also relatively low. This is a direct consequence of the NLO $\chi$PT description we are using.

## VI. DISCUSSION AND SUMMARY

In this paper, the isospin-0 $\pi\pi$ scattering is studied with Lüscher's finite volume formalism in twisted mass lattice QCD. We use a mixed action approach with the OS action in the valence sector to circumvent the complications arising from isospin symmetry breaking in the twisted mass quark action. The stochastic LapH quark smearing method is used to compute all-to-all quark propagators, which are required to compute the quark disconnected diagrams contributing to the isospin-0 $\pi\pi$ correlation function. The lowest energy level in the rest frame is extracted for three $N_f = 2$ ensembles with three different pion mass values. The scattering length is computed with Lüscher's formula for the two ensembles with the lowest

pion mass values. For the third ensemble with the largest pion mass value the scattering length cannot be determined reliably. In the computation of the scattering length we include the $\mathcal{O}(k^2)$ term in the effective range expansion using values for the effective range, which we compute using $\chi$PT. The chiral extrapolation of $M_\pi a_0^{I=0}$ is performed using NLO $\chi$PT. Extrapolated to the physical value of $M_\pi/f_\pi$, our result is $M_\pi a_0^{I=0} = 0.198(9)(6)$, which is compatible within errors with the newer experimental and theoretical determinations available in the literature.

Since we work at a single lattice spacing value only, we cannot estimate lattice artefacts in our result. In particular, we cannot exclude that our result is affected by residual systematic uncertainties stemming from unitarity breaking, which will vanish in the continuum limit. Moreover, the control over higher order contributions from $\chi$PT is rather limited. We cannot exclude that such contributions are sizable.

For these reasons a future study should include several lattice spacing values and ideally ensembles at the physical point. In order to avoid isospin breaking and unitarity breaking effects, we will repeat this computation with an action without isospin breaking.

## ACKNOWLEDGMENTS

We thank the members of ETMC for the most enjoyable collaboration. The computer time for this project was made available to us by the John von Neumann-Institute for Computing (NIC) on the Jureca and Juqueen systems in Jülich. We thank A. Rusetsky and Zhi-Hui Guo for very useful discussions and R. Briceño for valuable comments. We are grateful to Ulf-G. Meißner for carefully reading this manuscript and helpful comments. This project was funded by the DFG as a project in the Sino-German CRC110. S. B. has received funding from the Horizon 2020 research and innovation program of the European Commission under the Marie Sklodowska-Curie programme GrantNo. 642069. This work was granted access to the HPC resources IDRIS under the allocation 52271 made by GENCI. The open source software packages tmLQCD [49], Lemon [50], DD$\alpha$AMG [51] and R [52] have been used.

## APPENDIX A: EFFECTIVE RANGE FROM $\chi$PT

In order to investigate the contribution of the $\mathcal{O}(k^2)$ term in the effective range expansion, we need to know the value of the effective range $r_0$. As explained in Sec. V A, we estimate $r_0$ from $\chi$PT.

In Ref. [2], the chiral expansion of the threshold parameter $b_0^0$ to NLO is given as

$$b_0^0 = \frac{1}{2\pi f_\pi^2}\left\{1 + \frac{M_\pi^2}{f_\pi^2}\left[-\frac{13}{12\pi^2}\ln\frac{M_\pi^2}{\mu^2} + 32l_1^r + 24l_2^r + 4l_4^r - \frac{13}{96\pi^2}\right]\right\}, \tag{A1}$$

where $\mu$ is the renormalization scale, $l_1^r$, $l_2^r$ and $l_4^r$ are the renormalized, quark mass independent couplings. In this expression, we have replaced the low energy parameters $M$ and $F$ with their (lattice) physical values $M_\pi$ and $f_\pi$ using the NLO chiral expansions of $M_\pi^2$ and $f_\pi$, which are given in the same reference. Please also note that our convention of $f_\pi$ (∼130 MeV) is different from the $F_\pi$ (∼92.4 MeV) used in Ref. [2].

The effective range $r_0$ is related to $b_0^0$ as $r_0 = -2b_0^0 M_\pi$. In order to avoid the uncertainty in lattice scale setting, we write $r_0$ in lattice units as a function of the dimensionless parameters $aM_\pi$ and $M_\pi^2/f_\pi^2$:

$$\begin{aligned}\frac{r_0}{a} &= -\frac{2b_0^0 M_\pi^2}{aM_\pi} \\ &= -\frac{1}{aM_\pi}\frac{M_\pi^2}{\pi f_\pi^2}\left\{1 + \frac{M_\pi^2}{f_\pi^2}\left[-\frac{13}{12\pi^2}\ln\frac{M_\pi^2}{f_\pi^2} + 32l_1^r + 24l_2^r + 4l_4^r - \frac{13}{96\pi^2}\right]\right\}.\end{aligned}$$

Here the renormalization scale $\mu$ is set to be the physical pion decay constant $f_\pi^{\rm phy}$. To write the formula as a function of $M_\pi/f_\pi$, we have replaced $f_\pi^{\rm phy}$ with $f_\pi$. The corrections due to this replacement appear at next-to-next-to-leading order.

We take the values of the scale independent couplings $\bar{l}_1$, $\bar{l}_2$ and $\bar{l}_4$ determined in Ref. [53]:

$$\bar{l}_1 = -0.4 \pm 0.6, \qquad \bar{l}_2 = 4.3 \pm 0.1, \qquad \bar{l}_4 = 4.3 \pm 0.3. \tag{A2}$$

From the relations between $l_i^r$ and $\bar{l}_i$

$$l_i^r = \frac{\gamma_i}{32\pi^2}\left(\bar{l}_i + \ln\frac{M_\pi^2}{\mu^2}\right) \tag{A3}$$

with $\gamma_1 = 1/3$, $\gamma_2 = 2/3$ and $\gamma_4 = 2$, we calculate the values of $l_i^r$ at $\mu = f_\pi^{\rm phy}$:

$$l_1^r = -0.0003(6), \quad l_2^r = 0.0094(2), \quad l_4^r = 0.0281(19). \tag{A4}$$

The effective range is calculated with the $l_i^r$'s in Eq. (A4) and the values of $aM_\pi^{\rm OS}$ and $M_\pi^{\rm OS}/f_\pi^{\rm OS}$ in Table II and Table III. The results of $r_0/a$ for the three ensembles are presented in Table VI. The errors are estimated from the

TABLE VI. The effective range in lattice unit.

| Ensemble | cA2.09.48 | cA2.30.48 | cA2.60.32 |
|---|---|---|---|
| $r_0/a$ | −14.9(0.8) | −17(1) | −20(2) |

errors of $l_i^r$'s and the statistical uncertainties of $aM_\pi^{\mathrm{OS}}$ and $M_\pi^{\mathrm{OS}}/f_\pi^{\mathrm{OS}}$.

## APPENDIX B: DETERMINATION OF THE OS $f_\pi$ VALUES

The chiral extrapolation of the $I = 0$ scattering length is most conveniently performed in $M_\pi/f_\pi$. For this reason we need to compute also the OS pion decay constant. It is given by the following relation [54]

$$f_\pi^{\mathrm{OS}} = Z_A \frac{\langle 0|A_0|\pi\rangle}{M_\pi^{\mathrm{OS}}}, \tag{B1}$$

with the (OS valence quark) axial vector component $A_0 = \bar{u}\gamma_5\gamma_0 d$. The corresponding renormalization constant $Z_A$ has been determined in Ref. [55] for the action and $\beta$-value used here. It reads

$$Z_A = 0.7910(6).$$

The matrix element $\langle 0|A_0|\pi\rangle$ can be determined from suitable correlation functions. We used the operator

$$\mathcal{O}_A = \sum_{\mathbf{x}} \bar{u}\,\gamma_5\gamma_0 d(\mathbf{x}, t)$$

together with $\pi^+$ from Eq. (10) to build a $2 \times 2$ correlation matrix. For the matrix element we need local operators, hence, we cannot use sLapH. Instead, we performed dedicated inversions with local operators and the one-end-trick [56]. Since the off-diagonal correlators have a sinh-like behavior, we perform a constrained fit to this correlator matrix to determine the ground state energy and the corresponding matrix element at large Euclidean times.


[1] S. Weinberg, Physica A (Amsterdam) **96**, 327 (1979).
[2] J. Gasser and H. Leutwyler, Ann. Phys. (N.Y.) **158**, 142 (1984).
[3] J. Gasser and H. Leutwyler, Phys. Lett. B **188**, 477 (1987).
[4] S. Weinberg, Phys. Rev. Lett. **17**, 616 (1966).
[5] J. R. Batley *et al.* (NA48-2 Collaboration), Eur. Phys. J. C **70**, 635 (2010).
[6] S. Pislak *et al.*, Phys. Rev. D **67**, 072004 (2003); **81**, 119903 (E) (2010).
[7] J. R. Pelaez, Phys. Rep. **658**, 1 (2016).
[8] M. Lüscher, Commun. Math. Phys. **105**, 153 (1986).
[9] M. Lüscher, Nucl. Phys. **B354**, 531 (1991).
[10] T. Yagi, S. Hashimoto, O. Morimatsu, and M. Ohtani, arXiv:1108.2970.
[11] Z. Fu, Phys. Rev. D **87**, 074501 (2013).
[12] K. Sasaki, N. Ishizuka, M. Oka and T. Yamazaki (PACS-CS Collaboration), Phys. Rev. D **89**, 054502 (2014).
[13] C. Helmes, C. Jost, B. Knippschild, L. Liu, C. Urbach, M. Ueding, M. Werner, C. Liu, J. Liu, and Z. Wang (ETM Collaboration), J. High Energy Phys. 09 (2015) 109.
[14] R. A. Briceno, J. J. Dudek, R. G. Edwards, and D. J. Wilson, Phys. Rev. Lett. **118**, 022002 (2017).
[15] R. Frezzotti, P. A. Grassi, S. Sint and P. Weisz (ALPHA Collaboration), J. High Energy Phys. 08 (2001) 058.
[16] M. I. Buchoff, J.-W. Chen, and A. Walker-Loud, Phys. Rev. D **79**, 074503 (2009).
[17] R. Frezzotti and G. C. Rossi, J. High Energy Phys. 10 (2004) 070.
[18] Y. Iwasaki, Nucl. Phys. **B258**, 141 (1985).
[19] A. Abdel-Rehim *et al.* (ETM Collaboration), Phys. Rev. D **95**, 094515 (2017).
[20] R. Baron *et al.* (ETM Collaboration), J. High Energy Phys. 06 (2010) 111.
[21] B. Sheikholeslami and R. Wohlert, Nucl. Phys. **B259**, 572 (1985).
[22] T. Chiarappa, F. Farchioni, K. Jansen, I. Montvay, E. E. Scholz, L. Scorzato, T. Sudmann, and C. Urbach, Eur. Phys. J. C **50**, 373 (2007).
[23] R. Frezzotti and G. C. Rossi, J. High Energy Phys. 08 (2004) 007.
[24] K. Ottnad, C. Urbach and F. Zimmermann (ETM Collaboration), Nucl. Phys. **B896**, 470 (2015).
[25] C. Michael, K. Ottnad and C. Urbach (ETM Collaboration), Phys. Rev. Lett. **111**, 181602 (2013).
[26] C. W. Bernard, M. Golterman, J. Labrenz, S. R. Sharpe, and A. Ukawa, Nucl. Phys. B, Proc. Suppl. **34**, 334 (1994).
[27] C. Aubin, J. Laiho, and R. S. Van de Water, Phys. Rev. D **77**, 114501 (2008).
[28] W. A. Bardeen, A. Duncan, E. Eichten, N. Isgur, and H. Thacker, Phys. Rev. D **65**, 014509 (2001).
[29] M. Golterman, T. Izubuchi, and Y. Shamir, Phys. Rev. D **71**, 114508 (2005).
[30] C. W. Bernard and M. F. L. Golterman, Phys. Rev. D **53**, 476 (1996).
[31] M. Peardon, J. Bulava, J. Foley, C. Morningstar, J. Dudek, R. G. Edwards, B. Joó, H.-W. Lin, D. G. Richards, and K. J. Juge (Hadron Spectrum Collaboration), Phys. Rev. D **80**, 054506 (2009).
[32] C. Morningstar, J. Bulava, J. Foley, K. J. Juge, D. Lenkner, M. Peardon, and C. H. Wong, Phys. Rev. D **83**, 114505 (2011).
[33] X. Feng, K. Jansen, and D. B. Renner, Phys. Lett. B **684**, 268 (2010).
[34] C. Michael and I. Teasdale, Nucl. Phys. **B215**, 433 (1983).
[35] H. Neff, N. Eicker, T. Lippert, J. W. Negele, and K. Schilling, Phys. Rev. D **64**, 114509 (2001).

[36] K. Jansen, C. Michael and C. Urbach (ETM Collaboration), Eur. Phys. J. C **58**, 261 (2008).
[37] P. Dimopoulos, R. Frezzotti, C. Michael, G. C. Rossi, and C. Urbach, Phys. Rev. D **81**, 034509 (2010).
[38] M. Albaladejo and J. A. Oller, Phys. Rev. D **86**, 034003 (2012).
[39] J. R. Pelaez and G. Rios, Phys. Rev. D **82**, 114002 (2010).
[40] C. Hanhart, J. R. Pelaez, and G. Rios, Phys. Rev. Lett. **100**, 152001 (2008).
[41] C.Hanhart (private communication).
[42] V. Bernard, M. Lage, U. G. Meissner, and A. Rusetsky, J. High Energy Phys. 01 (2011) 019.
[43] M. Doring, U.-G. Meissner, E. Oset, and A. Rusetsky, Eur. Phys. J. A **47**, 139 (2011).
[44] J. Bijnens, G. Colangelo, G. Ecker, J. Gasser, and M. Sainio, Nucl. Phys. **B508**, 263 (1997).
[45] J. Bijnens, G. Colangelo, G. Ecker, J. Gasser, and M. E. Sainio, Phys. Lett. B **374**, 210 (1996).
[46] G. Colangelo, J. Gasser, and H. Leutwyler, Nucl. Phys. **B603**, 125 (2001).
[47] A. Walker-Loud, arXiv:0904.2404.
[48] C. Hanhart, J. R. Pelaez, and G. Rios, Phys. Lett. B **739**, 375 (2014).
[49] K. Jansen and C. Urbach, Comput. Phys. Commun. **180**, 2717 (2009).
[50] A. Deuzeman, S. Reker and C. Urbach (ETM Collaboration), Comput. Phys. Commun. **183**, 1321 (2012).
[51] C. Alexandrou, S. Bacchio, J. Finkenrath, A. Frommer, K. Kahl, and M. Rottmann, Phys. Rev. D **94**, 114509 (2016).
[52] R Development Core Team, *R: A Language and Environment for Statistical Computing* (R Foundation for Statistical Computing, Vienna, Austria, 2005), 3-900051-07-0.
[53] J. Bijnens and G. Ecker, Annu. Rev. Nucl. Part. Sci. **64**, 149 (2014).
[54] M. Constantinou *et al.* (ETM Collaboration), J. High Energy Phys. 08 (2010) 068.
[55] C. Alexandrou, M. Constantinou and H. Panagopoulos (ETM Collaboration), Phys. Rev. D **95**, 034505 (2017).
[56] P. Boucaud *et al.* (ETM Collaboration), Comput. Phys. Commun. **179**, 695 (2008).